Interaction of electromagnetic field with electrons in a Wigner crystal

Z. Lenac
Department of Physics, University of Rijeka, 51000 Rijeka, Croatia
(Received 7 July 2004; revised manuscript received 1 November 2004; published 21 January 2005)

The interaction between electrons that form a quasi-two-dimensional crystal, as well as their interaction with a dielectric/metallic substrate (image potential), is well understood within the standard theory of Wigner crystals. Here we analyze the influence of the quantized electromagnetic field on the dynamics of Wigner electrons, i.e., on the dispersion relation of Wigner phonons. We have found that a significant influence can be expected from the surface polariton field when the energies of the surface polaritons and Wigner phonons coincide. Such polaritons can be expected in ionic crystals or doped semiconductors and we have proposed a geometry that can lead to the detection of a Wigner crystal by measuring the dispersion relation of surface polaritons.

DOI: 10.1103/PhysRevB.71.035330 PACS number(s): 73.20.Qt, 73.20.Mf, 78.68.+m

I. INTRODUCTION

The Coulomb interaction between electrons at low electron densities is responsible for the formation of a quasi-two-dimensional crystal, because electrons have lower energy oscillating around the lattice points than in the gas phase. The energy difference is very small, therefore a crystal such as this is stable only at very low temperatures. Its existence was theoretically predicted by Wigner,[1] but experimental preparation was (and still remains) a rather tedious task mainly because one has to prevent dissolution of Wigner electrons into the substrate. The crystal was observed for the first time by Grimes and Adams,[2] who trapped electrons on a liquid He layer, which has an energy gap at the typical energies of Wigner electrons. The explanation of the excitation spectrum was given by Fisher *et al.*[3] and it includes the interaction between phonons of a Wigner lattice and capillary waves (ripplons) of a He substrate. This interaction becomes significant at very low phonon energies and small wave vectors involved in the experiment.[4]

There is an obvious question: Do Wigner phonons follow the unperturbed, well known dispersion relation at higher frequencies and wave vectors, or should one take into account yet another interaction? A promising candidate would be the electron-photon interaction. But here we are not interested in a "direct" interaction, i.e., the excitation of a single electron in some higher perpendicular state.[5] Rather we would like to analyze the interaction of Wigner phonons with the electromagnetic field and discuss the possible change in the corresponding phonon and photon dispersion relations. It is well known that the standard photon-phonon interaction dominantly involves only small phonon wave vectors. However, in the case of a Wigner crystal, one should take into account also the interaction between phonons and surface polaritons (SP's), which are the coupled modes of the electromagnetic field and the charged particles in the dielectric (metallic) substrate. The SP dispersion relation is similar in shape to the phonon dispersion relation so if they eventually fall in the same energy range, we could expect a strong interaction between these excitations. In order to have a complete theory, we shall also include the interaction with ripplons. In such an approach, we need a quantized form of the phonon, polariton, and ripplon fields and the appropriate transformation that could define the renormalized frequencies.

The article is organized as follows. In Sec. II we first briefly discuss the Hamiltonian of Wigner phonons, without an interaction with external fields. Then we analyze the appropriate Hamiltonian of the electromagnetic field and the photon-phonon interaction. Next, the ripplon Hamiltonian and the phonon-ripplon coupling are added. Finally, the diagonalization of the total Hamiltonian leads to the required form of the renormalized phonon eigenfrequencies. The results are discussed in Sec. III, and the conclusion is given in Sec. IV.

II. EIGENMODES OF A WIGNER CRYSTAL

The properties of a Wigner crystal are usually analyzed by taking into account the Coulomb interaction among crystal electrons,[6] possibly adding the influence of the image potential due to the metallic substrate.[7] Here we wish to determine the eigenmodes of Wigner electrons that also interact with photon and ripplon fields. Let us start to analyze those fields one by one, and then add the interaction.

A. Wigner crystal

The Hamiltonian of a Wigner crystal above a flat (liquid He) surface can be put in the form[6,7]

$$H_{Wig} = H_{osc} + \langle E_{im} \rangle + \langle W_{ee} \rangle. \tag{1}$$

H_{osc} describes the *parallel* oscillation of Wigner electrons (Wigner phonons). $\langle E_{im} \rangle$ represents the averaged perpendicular kinetic energy as well as the averaged interaction of each electron with the substrate (*image potential*), and $\langle W_{ee} \rangle$ is the averaged interaction between electrons at their regular lateral sites.

The averaged values are obtained by using the perpendicular wave function that describes electrons in their perpendicular ground state,[7]

$$u(z) = 2a^{3/2} z e^{-az}, \quad z > 0 \tag{2}$$

with the damping parameter $a = 3/2z_0$, and z_0 is the mean perpendicular position of electrons above the substrate.

Here we are interested in the dynamics of the Wigner crystal, given by[6,7]

$$H_{osc} = \sum_{\mu\boldsymbol{\kappa}} \hbar\Omega^0_{\mu\boldsymbol{\kappa}}(b^\dagger_{\mu\boldsymbol{\kappa}} b_{\mu\boldsymbol{\kappa}} + \tfrac{1}{2}). \tag{3}$$

$\Omega^0_{\mu\boldsymbol{\kappa}}$ are the eigenfrequencies of Wigner phonons, determined by the two-dimensional phonon wave vector $\boldsymbol{\kappa}$ from the first Brillouin zone, and the polarization μ that can be either longitudinal (L) or transverse (T). $b^\dagger_{\mu\boldsymbol{\kappa}}$ and $b_{\mu\boldsymbol{\kappa}}$ are the standard creation and annihilation operators of phonons, respectively.

We assume that Wigner electrons form a quasi-two-dimensional hexagonal (triangular) lattice with the reciprocal lattice vector $\mathbf{G}$. The primitive lattice vector in the reciprocal space is given by $g_0 = 4\pi/\sqrt{3}r_0$ and r_0 is the lattice constant related to the surface electron density by $n_s = 2/\sqrt{3}r_0^2$. Other reciprocal vectors can be calculated from

$$G_{mn} = g_0\sqrt{m^2 + n^2 - mn}, \quad \{m,n\} = 0, \pm 1, \pm 2, \pm 3, \ldots,$$

The existence of a Wigner crystal is predicted from the first principles[8] as well as from the model calculations[9] at $r_0 > 40$ Å, although some recent theories allow it even at higher densities.[10] Here we are interested in a high-density region ($r_0 \approx 50$ Å) since at these densities the phonon frequencies are comparable with the SP spectrum. Notice that relevant experiments to date were done at lower electron densities.[2,11,12] Also notice that at very low electron densities a square lattice can be more favorable than the hexagonal lattice.[13]

B. Photons

Let us briefly discuss the electromagnetic field in a dispersive dielectric media with a planar symmetry, so that each layer l is described by a dielectric function ϵ_l. The vector potential takes a standard form:[14,15]

$$\mathbf{A}(\mathbf{r}) = \frac{1}{\sqrt{A_s}} \sum_{\nu\mathbf{k}\beta} \zeta_{\beta\mathbf{k}} [\mathbf{A}^\beta_{\nu\mathbf{k}}(z) a^\beta_{\nu\mathbf{k}} + \mathbf{A}^{\beta *}_{\nu-\mathbf{k}}(z) a^{\beta\dagger}_{\nu-\mathbf{k}}] e^{i\mathbf{k}\cdot\boldsymbol{\rho}}. \tag{4}$$

Here A_s denotes the normalization surface, and ζ is the normalization parameter:

$$\zeta_{\beta\mathbf{k}} = c\sqrt{h/\omega_{\beta\mathbf{k}}}.$$

The time dependence is implicitly assumed, i.e., the polariton annihilation operator $a^\beta_{\nu\mathbf{k}}$ oscillates in time with the eigenfrequency $\omega_{\beta\mathbf{k}}$.

The eigenmodes of the vector potential $\mathbf{A}^\beta_{\nu\mathbf{k}}(z)$ are determined by the two-dimensional wave vector $\mathbf{k}$, the "perpendicular wave vector" β, defined as $\beta^2 = \epsilon\omega^2_{\beta\mathbf{k}}/c^2 - k^2$, and by the polarization ν, which can be either p (in the plane of incidence) or s (in the direction perpendicular to the plane of incidence). The eigenfrequencies $\omega_{\beta\mathbf{k}}$ are determined by the eigenequation

$$\boldsymbol{\nabla} \times \boldsymbol{\nabla} \times \mathbf{A}^\beta_{\nu\mathbf{k}}(z) e^{i\mathbf{k}\cdot\boldsymbol{\rho}} - \frac{1}{c^2}\epsilon\omega^2_{\beta\mathbf{k}} \mathbf{A}^\beta_{\nu\mathbf{k}}(z) e^{i\mathbf{k}\cdot\boldsymbol{\rho}} = \mathbf{0}. \tag{5}$$

Let us assume that $\epsilon = \epsilon(\omega_{\beta\mathbf{k}})$ is a real, Lorentz-type dielectric function of a medium, or it takes a constant value for an inert dielectric. Using that model, we can put the Hamiltonian of a photon field in a dispersive dielectric media (usually called a *polariton* field) in a diagonal form:[15]

$$H_{ph} = \sum_{\nu\mathbf{k}\beta} \hbar\omega_{\beta\mathbf{k}} (a^{\beta\dagger}_{\nu\mathbf{k}} a^\beta_{\nu\mathbf{k}} + \tfrac{1}{2}). \tag{6}$$

C. Electron-photon interaction

The interaction between the electromagnetic field and the electrons of a Wigner lattice at positions $\mathbf{r}_j$ and with momenta $\mathbf{p}_j$, is described in a standard way:

$$H_{int} = H_{pA} + H_{AA},$$

$$H_{pA} = -\frac{e}{mc} \sum_j \langle \mathbf{p}_j \cdot \mathbf{A}(\mathbf{r}_j) \rangle, \tag{7}$$

$$H_{AA} = \frac{e^2}{2mc^2} \sum_j \langle \mathbf{A}(\mathbf{r}_j) \cdot \mathbf{A}(\mathbf{r}_j) \rangle, \tag{8}$$

where $\langle\ \rangle$ means that we have to take the average with the perpendicular electron wave function $u(z)$, Eq. (2). We shall also assume that the vector potential is taken at the regular lateral position of Wigner electrons $\boldsymbol{\rho}^0_j$, i.e., $\mathbf{r}_j = \boldsymbol{\rho}^0_j + z\hat{\mathbf{z}}$ (*dipole approximation*).

The two-photon processes are described by H_{AA}, Eq. (8), which, after inserting the expansion (4), becomes:

$$H_{AA} = \frac{e^2 n_s}{2mc^2} \sum_\nu \sum_{\beta\beta'} \sum_{\mathbf{k}\mathbf{G}'} \zeta_{\beta\mathbf{k}}\zeta_{\beta'\mathbf{k}'} \langle [a^\beta_{\nu\mathbf{k}} \mathbf{A}^\beta_{\nu\mathbf{k}}(z) + a^{\beta\dagger}_{\nu-\mathbf{k}} \mathbf{A}^{\beta *}_{\nu-\mathbf{k}}(z)]$$
$$\times [a^{\beta'}_{\nu-\mathbf{k}'} \mathbf{A}^{\beta'}_{\nu-\mathbf{k}'}(z) + a^{\beta'\dagger}_{\nu\mathbf{k}'} \mathbf{A}^{\beta' *}_{\nu\mathbf{k}'}(z)] \rangle,$$

where $\mathbf{k}' = \mathbf{k} + \mathbf{G}'$.

The electron momentum $\mathbf{p}_j$ can be divided into parallel $\mathbf{p}^\parallel_j$ and perpendicular $\mathbf{p}^\perp_j$ components. We find

$$\langle \mathbf{p}^\perp_j \rangle = 0,$$

$$\langle \mathbf{p}^\parallel_j \rangle = \frac{1}{\sqrt{A_s}} \sum_{\mu\boldsymbol{\kappa}} (-i)\, \eta_{\mu\boldsymbol{\kappa}} [b_{\mu-\boldsymbol{\kappa}} - b^\dagger_{\mu\boldsymbol{\kappa}}] \mathbf{e}^*_{\mu\boldsymbol{\kappa}} e^{-i\boldsymbol{\kappa}\cdot\boldsymbol{\rho}^0_j},$$

where $\mathbf{e}_{\mu\boldsymbol{\kappa}}$ is the unit polarization vector, and

$$\eta_{\mu\boldsymbol{\kappa}} = \sqrt{\hbar m \Omega^0_{\mu\boldsymbol{\kappa}}/2}.$$

Now the Hamiltonian H_{pA}, Eq. (7), can be put in the form

$$H_{pA} = i\frac{e}{mc} \sum_{\mu\nu} \sum_{\mathbf{k}\beta} \sqrt{n_s}\, \eta_{\mu\boldsymbol{\kappa}} \zeta_{\beta\mathbf{k}} \langle [\mathbf{e}^*_{\mu\boldsymbol{\kappa}} \cdot \mathbf{A}^\beta_{\nu\mathbf{k}}(z) a^\beta_{\nu\mathbf{k}}$$
$$+ \mathbf{e}^*_{\mu\boldsymbol{\kappa}} \cdot \mathbf{A}^{\beta *}_{\nu-\mathbf{k}}(z) a^{\beta\dagger}_{\nu-\mathbf{k}}] \rangle [b_{\mu-\boldsymbol{\kappa}} - b^\dagger_{\mu\boldsymbol{\kappa}}].$$

The summations extend over all perpendicular (β) and parallel wave vectors $\mathbf{k} = \boldsymbol{\kappa} + \mathbf{G}$ as well as over the phonon (μ) and the photon (ν) polarizations.

Let us divide the vector potential into the perpendicular part $\mathbf{A}^\perp$ (with the perpendicular component of p polarization $\nu = p_\perp$) and the lateral part $\mathbf{A}^\parallel$ (with the parallel polarizations $\nu = \{s, p_\parallel\}$):

$$\mathbf{A}^{\beta}_{\nu\mathbf{k}}(z) = \mathbf{A}^{\beta\perp}_{\nu\mathbf{k}}(z) + \mathbf{A}^{\beta\|}_{\nu\mathbf{k}}(z). \quad (9)$$

Now we shall assume that the longitudinal polarization $\mu = L$ of phonons takes the same direction ($\boldsymbol{\kappa}$) as the parallel component of *p*-polarized photons, for all wave vectors $\boldsymbol{\kappa}$ (it is strictly correct for $\kappa \ll g_0$). Therefore the *T*-polarized phonons are assumed to propagate in the same direction as the *s*-polarized photons, and we can write

$$\mathbf{e}^{*}_{\mu\boldsymbol{\kappa}} \cdot \mathbf{A}^{\beta}_{\nu\mathbf{k}}(z) = \mathbf{A}^{\beta\|}_{\mu\mathbf{k}}(z)\,\delta_{\mu,\nu}.$$

From now on we shall neglect the influence of the perpendicular component $\mathbf{A}^{\perp}$ on the (lateral) phonon frequencies of the Wigner lattice, which shall be stressed by using the same polarization index $\mu = (L,T)$ for both phonon and photon modes.

The Hamiltonian H^{ph}_{osc} that includes photons, Wigner phonons, and their interaction,

$$H^{ph}_{osc} = H_{osc} + H_{ph} + H_{int}, \quad (10)$$

can be diagonalized with the generalized Hopfiled transformation,[16,17]

$$d_{\mu\boldsymbol{\kappa}} = u_{\mu\boldsymbol{\kappa}} b_{\mu\boldsymbol{\kappa}} + v_{\mu\boldsymbol{\kappa}} b^{\dagger}_{\mu\boldsymbol{\kappa}} + \sum_{\beta\mathbf{G}} \left[Y^{\beta}_{\mu\mathbf{k}} a^{\beta}_{\mu\mathbf{k}} + Z^{\beta}_{\mu\mathbf{k}} a^{\beta\dagger}_{\mu\mathbf{k}} \right],$$

where the summation extends over all perpendicular wave vectors β and over all $\mathbf{G}$ components of the parallel wave vector $\mathbf{k} = \boldsymbol{\kappa} + \mathbf{G}$. The new operator $d_{\mu\boldsymbol{\kappa}}$ involves four parameters (u,v,Z,Y) which should be determined by the following requirement:

$$[d_{\mu\boldsymbol{\kappa}}, H^{ph}_{osc}] = \hbar \Omega^{ph}_{\mu\boldsymbol{\kappa}} d_{\mu\boldsymbol{\kappa}},$$

where $\Omega^{ph}_{\mu\boldsymbol{\kappa}}$ is the renormalized phonon frequency due to the phonon-photon interaction. This requirement leads us to the four equations:

$$\hbar(\Omega^{ph}_{\mu\boldsymbol{\kappa}} - \Omega^{0}_{\mu\boldsymbol{\kappa}}) u_{\mu\boldsymbol{\kappa}} = i \frac{e}{mc} \sqrt{n_s}\, \eta^{*}_{\mu\boldsymbol{\kappa}} \mathbf{e}_{\mu\boldsymbol{\kappa}} \cdot \mathbf{F}_{\mu\boldsymbol{\kappa}},$$

$$\hbar(\Omega^{ph}_{\mu\boldsymbol{\kappa}} + \Omega^{0}_{\mu\boldsymbol{\kappa}}) v_{\mu\boldsymbol{\kappa}} = -i \frac{e}{mc} \sqrt{n_s}\, \eta^{*}_{\mu\boldsymbol{\kappa}} \mathbf{e}_{\mu\boldsymbol{\kappa}} \cdot \mathbf{F}_{\mu\boldsymbol{\kappa}},$$

$$\hbar(\Omega^{ph}_{\mu\boldsymbol{\kappa}} - \omega^{\beta}_{\mu\mathbf{k}}) Y^{\beta}_{\mu\mathbf{k}} = -i \frac{e}{mc} \sqrt{n_s}\, \eta_{\mu\boldsymbol{\kappa}} \zeta_{\beta\mathbf{k}} \mathbf{e}^{*}_{\mu\boldsymbol{\kappa}} \cdot \mathbf{A}^{\beta}_{\mu\mathbf{k}} (u_{\mu\boldsymbol{\kappa}} + v_{\mu\boldsymbol{\kappa}}) + \sqrt{\frac{e^2 n_s}{mc^2}}\, \zeta_{\beta\mathbf{k}} \mathbf{A}^{\beta}_{\mu\mathbf{k}} \cdot \mathbf{F}_{\mu\boldsymbol{\kappa}},$$

$$\hbar(\Omega^{ph}_{\mu\boldsymbol{\kappa}} + \omega^{\beta}_{\mu\mathbf{k}}) Z^{\beta}_{\mu\mathbf{k}} = -i \frac{e}{mc} \sqrt{n_s}\, \eta_{\mu\boldsymbol{\kappa}} \zeta_{\beta\mathbf{k}} \mathbf{e}_{\mu\boldsymbol{\kappa}} \cdot \mathbf{A}^{\beta^{*}}_{\mu-\mathbf{k}} (u_{\mu\boldsymbol{\kappa}} + v_{\mu\boldsymbol{\kappa}}) + \sqrt{\frac{e^2 n_s}{mc^2}}\, \zeta_{\beta\mathbf{k}} \mathbf{A}^{\beta}_{\mu\mathbf{k}} \cdot \mathbf{F}_{\mu\boldsymbol{\kappa}},$$

where we have introduced

$$\mathbf{F}_{\mu\boldsymbol{\kappa}} = \sum_{\beta\mathbf{G}} \zeta_{\beta\mathbf{k}} (\mathbf{A}^{\beta}_{\mu\mathbf{k}} Y^{\beta}_{\mu\mathbf{k}} - \mathbf{A}^{\beta}_{\mu-\mathbf{k}} Z^{\beta}_{\mu\mathbf{k}}).$$

After the straightforward calculation the above-mentioned equations can be combined to give the dispersion relation for the renormalized phonon frequencies:

$$\Omega^{ph2}_{\mu\boldsymbol{\kappa}} - \Omega^{02}_{\mu\boldsymbol{\kappa}} = 4\pi \frac{e^2 n_s}{m} \sum_{\beta\mathbf{G}} \frac{\Omega^{ph2}_{\mu\boldsymbol{\kappa}}}{\Omega^{ph2}_{\mu\boldsymbol{\kappa}} - \omega^{2}_{\beta\mathbf{k}}} \langle |\mathbf{A}^{\beta}_{\mu\mathbf{k}}(z)|^2 \rangle. \quad (11)$$

To calculate the electromagnetic field acting on Wigner electrons we have to define the properties of a medium that supports Wigner crystal. In a standard model, we assume that a Wigner crystal is formed above a liquid He layer which is deposited on a dielectric or metallic substrate. The electromagnetic field above the He surface, i.e., in the vacuum ($\epsilon_0 = 1$), can be divided according to the parameter $\beta_0^2 = \omega^2_{\beta\mathbf{k}}/c^2 - k^2$, into the radiative ($\beta_0^2 > 0$) and the surface ($\beta_0^2 < 0$) modes. Obviously, the radiative modes are real photons that could be involved, e.g., in the excitation of Wigner electrons, but they do not change Wigner phonon frequencies. If one tries to apply Eq. (11) to radiative modes, the right-hand side will diverge, which makes the whole procedure meaningless.

The surface modes have exponentially damped electromagnetic field above the He surface, with the damping parameter $\alpha_0 = -i\beta_0 = \sqrt{k^2 - \omega^2_{\beta\mathbf{k}}/c^2}$. Those modes are the result of the dynamics of ions in ionic crystal or conducting electrons in metals, where the electromagnetic field is coupled with such oscillations into the *surface polaritons*. Liquid He is not a polar medium and it can be described as an inert dielectric of a thickness d_h, with a dielectric constant $\epsilon_h = 1.057$. SP modes are therefore supported by the substrate below the He layer, and they will influence the Wigner electrons only if the effective distance of a Wigner crystal ($z_0 + d_h$) is not much larger than the attenuation parameter $1/\alpha_0$.

To be specific, let us assume that the He layer with a Wigner crystal on it, is supported by a thin dielectric film of a thickness d_i, deposited on a semi-infinite metal (Fig. 1). For the ionic crystal we shall take the standard dielectric function:

$$\epsilon_i(\omega) = \epsilon_\infty \frac{\omega_L^2 - \omega^2}{\omega_T^2 - \omega^2}, \quad (12)$$

with ω_L and ω_T being the longitudinal and the transverse frequency of the crystal, respectively. The dielectric function ϵ_m of the metallic substrate can be taken in the same form, with the usual replacement: $\omega_T \to 0$ and $\omega_L \to \omega_P$, where ω_P is the frequency of the electronic plasma in the metal. However, we are interested in the Wigner phonons whose frequencies are much lower than ω_P, so we can assume that the metallic plate perfectly screens the electromagnetic field ($\epsilon_m \to -\infty$).

From Eq. (5) we find the vector potential of SP eigenmodes above the ionic crystal:

$$\mathbf{A}^{\beta}_{p\mathbf{k}}(z) = C^{\beta}_{p} (-i\alpha_0 \hat{\mathbf{k}} + k\hat{\mathbf{z}}) e^{-\alpha_0 (d_h + z)},$$

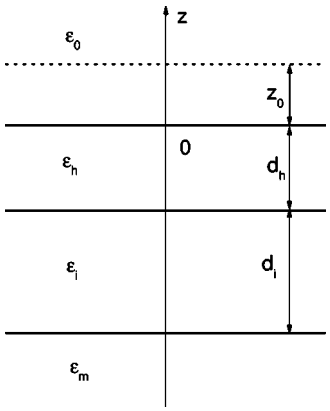

FIG. 1. Geometry of the model.

$$\mathbf{A}^{\beta}_{s\mathbf{k}}(z) = C^{\beta}_{s}(\hat{\mathbf{k}} \times \hat{\mathbf{z}})e^{-\alpha_0(d_h+z)}.$$

The SP eigenfrequencies as well as the normalization constants C^{β}_{p} and C^{β}_{s} are determined in the Appendix. After averaging with the function $u(z)$, Eq. (2), we find the matrix elements that determine the renormalized phonon frequencies in Eq. (11):

$$\langle|\mathbf{A}^{\beta}_{\mu\mathbf{k}}(z)|^2\rangle = |C^{\beta}_{\mu}|^2 e^{-2\alpha_0 d_h}\frac{1}{(1+\alpha_0/a)^3}\begin{cases}\alpha_0^2, & \mu = p_{\parallel}\\ 1, & \mu = s.\end{cases} \quad (13)$$

D. Ripplons

Capillary waves of a liquid He surface (*ripplons*) also interact with the vibrations of the Wigner lattice. Free ripplons have a dispersion relation:

$$\omega^2_{\mathbf{k}} = \frac{\alpha}{\rho}k^3,$$

where α and ρ are the surface tension and the density of the liquid He.

Due to the interaction with the liquid He substrate, the eigenfrequencies of the Wigner phonons $\Omega^{0}_{\mu\boldsymbol{\kappa}}$ are renormalized and the new frequencies $\Omega^{rp}_{\mu\boldsymbol{\kappa}}$ are determined from[3]

$$\Omega^{rp2}_{\mu\boldsymbol{\kappa}} - \Omega^{02}_{\mu\boldsymbol{\kappa}} = \frac{1}{2}\sum_{\mathbf{G}}\frac{\Omega^{rp2}_{\mu\boldsymbol{\kappa}}}{\Omega^{rp2}_{\mu\boldsymbol{\kappa}} - \omega^2_{\mathbf{k}}}|V_{\mathbf{k}}|2, \quad (14)$$

where again we have used the notation $\mathbf{k} = \boldsymbol{\kappa} + \mathbf{G}$. In the long-wavelength limit ($\kappa \ll g_0$) one can approximate $\mathbf{k} \approx \mathbf{G}$. The interaction matrix element is given by

$$V_{\mathbf{k}} = \sqrt{\frac{n_s}{m\alpha}}f(\mathbf{k})e^{-W(\mathbf{k})},$$

where $W(\mathbf{k})$ is the Debye-Waller factor of a Wigner lattice, and $f(\mathbf{k})$ is the effective force acting on Wigner electrons on the He substrate:[3,11]

$$f(\mathbf{k}) = eE_{\perp}(z_0) + \frac{1}{8}\frac{(\epsilon_h - 1)}{(\epsilon_h + 1)}e^2k^2\ln\left(\frac{1}{z_0 k}\right).$$

$E_{\perp}$ represents the perpendicular component of the electric field acting on the Wigner electrons.[3,7]

Here we are particularly interested in high frequencies at which Eq. (14) takes a simple form:

$$\Omega^{rp2}_{\mu\boldsymbol{\kappa}} \approx \Omega^{02}_{\mu\boldsymbol{\kappa}} + \Omega^{dp2}_{\boldsymbol{\kappa}}, \quad (15)$$

where

$$\Omega^{dp2}_{\boldsymbol{\kappa}} = \frac{1}{2}\sum_{\mathbf{G}}|V_{\boldsymbol{\kappa}+\mathbf{G}}|^2 \quad (16)$$

is a frequency of an electron in a static dimple. It shows a very small dispersion so it can be well approximated by $\Omega^{dp}_{\mathbf{0}}$.

E. Renormalized Wigner phonon frequencies

Obviously, the two equations (11) and (14) have the same form so we can combine them in order to obtain the dispersion relation for the Wigner phonos that includes the interaction with the He substrate as well as the interaction with the electromagnetic field:

$$\Omega^2_{\mu\boldsymbol{\kappa}} - \Omega^{02}_{\mu\boldsymbol{\kappa}} = \frac{e^2 n_s}{m}\sum_{\mathbf{G}}\left\{\frac{1}{2}|U_{\mathbf{k}}|^2\frac{\Omega^2_{\mu\boldsymbol{\kappa}}}{\Omega^2_{\mu\boldsymbol{\kappa}} - \omega^2_{\mathbf{k}}} + \sum_{\beta}4\pi|\mathbf{A}^{\beta}_{\mu\mathbf{k}}|^2\frac{\Omega^2_{\mu\boldsymbol{\kappa}}}{\Omega^2_{\mu\boldsymbol{\kappa}} - \omega^2_{\beta\mathbf{k}}}\right\}, \quad (17)$$

where we have introduced the renormalized phonon-ripplon interaction:

$$U_{\mathbf{k}} = \sqrt{\frac{m}{n_s e^2}}V_{\mathbf{k}} = \sqrt{\frac{1}{\alpha e^2}}f(\mathbf{k})e^{-W(\mathbf{k})}.$$

III. RESULTS AND DISCUSSION

We are now able to analyze the influence of the photons and ripplons on the frequencies of Wigner phonons. The influence of the ripplons at low frequencies (below $\Omega^{dp}_{\boldsymbol{\kappa}}$) is well known[3] so we shall be more interested in the influence of the photon spectrum, which becomes important at higher frequencies. Let us first analyze the possible influence of the metallic substrate. The typical frequency of SP in metals is $\omega_P/\sqrt{2}$. Usually we find $\omega_P > 1$ eV so the typical SP frequencies are much higher than the frequency spectrum of Wigner phonons, which lies below 0.1 eV. It means that one cannot expect a significant influence of the metal polaritons on the Wigner phonons, or vice versa. Obviously, the promising setup would be to put a thin dielectric layer with well defined optical phonons (ionic crystal), to support Wigner electrons. The SP in ionic crystals have the frequency spectrum between the transverse ω_T and the longitudinal ω_L frequency, and they typically lie below 0.1 eV. It means that one can expect a "crossing" between the polariton and phonon dispersion curves, that could cause their significant change. For the experimental reasons, one usually puts a thin liquid He layer below the Wigner crystal in order to prevent the penetration of Wigner electrons into the substrate. Therefore, our setup, as shown on Fig. 1, consists of Wigner crystal, inert dielectric layer (liquid He), optically active dielectric layer, and metallic substrate (the electrode).

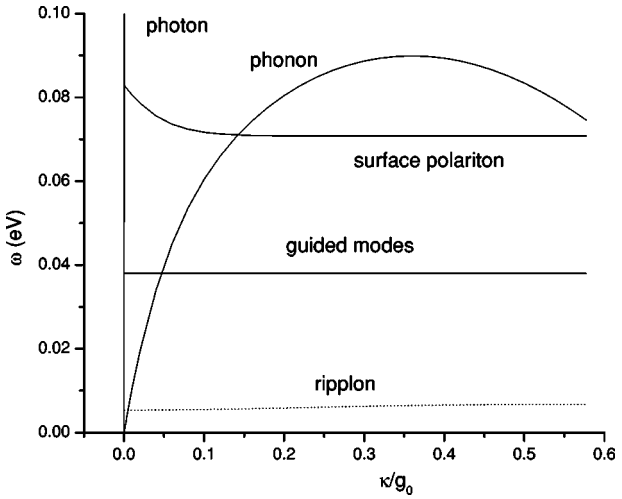

FIG. 2. Dispersion relation of free fields.

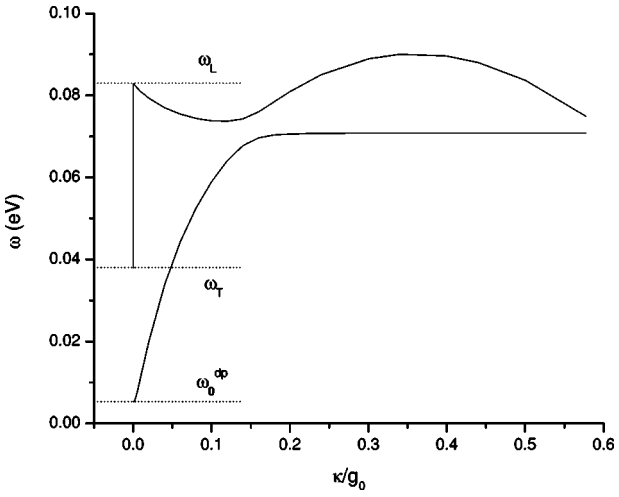

FIG. 3. Dispersion relation of coupled fields.

Let us first analyze the dispersion relations for free surface polaritons, ripplons, and Wigner phonons, as shown on Fig. 2. The SP curve is calculated from Eq. (A1) given in the Appendix. We took LiF as a dielectric layer, with $\epsilon_\infty=1.9$, $\omega_T=0.038$ eV, $\omega_L=0.083$ eV. The layers' thickness is $d_h=100$ Å, $d_i=100$ Å, and the lattice parameter is $r_0=50$ Å ($g_0=0.145$ Å^{-1}). The self-consistent result for the mean perpendicular position of Wigner electrons is $z_0=6$ Å.

The SP mode is "connected" to the active-dielectric–inert dielectric interface ($z=-d_h$) and its asymptotic frequency follows from $(\epsilon_i+\epsilon_h)=0$. There is only a *p*-polarized SP mode, so here we analyze only longitudinal Wigner phonons. Note that only those phonons also strongly interact with ripplons. The guided modes, which electromagnetic field is exponentially damped into the vacuum but oscillates within the ionic crystal, are also shown. The (ω,κ) plane is taken to give the best view of the crossing between the phonon and SP curves, so the photon curve ($\omega=\kappa c$) looks almost parallel to the *y* axes and the ripplon curve [the frequency ω_κ^{bp}, Eq. (16), is shown] is almost parallel to the *x* axes. The photon and polariton curves are very close at small wave vectors. In fact, the SP curve starts with $\kappa_T=\omega_T/c$ and suddenly leaves the photon curve roughly at $\kappa_L=\omega_L/c$. It can be better seen in Fig. 3, where the polariton and the phonon curves are shown for the interacting system. In comparison with Fig. 2, one can observe two main changes: (i) due to the interaction with ripplons, the phonon curve starts from the frequency ω_0^{dp}, in agreement with Eq. (15); (ii) due to the interaction with surface polariton, a strong splitting occurs between the phonon and SP curves around the crossing point, as expected. This splitting could be clear evidence of existence of the Wigner lattice.

Obviously, the phonon curve also crosses the guided modes curves. These modes are shown on Fig. 2 as a straight line at the frequency $\omega_T=0.038$ eV. In fact, these modes [determined by Eq. (A2) in the Appendix], start below ω_T and there is an infinite number of them between the starting frequency and ω_T. But all their frequencies are very close to ω_T and, e.g., even at small wave vector $\kappa=0.01g_0$, we find for the three lowest frequencies: $\omega=\{3.799980, 3.799998, 3.799999\}\times10^{-2}$ eV. The dielectric constant at those frequencies becomes very large ($\epsilon_i>6.6\times10^5$), so the interaction between the Wigner phonon and guided modes is quite negligible, as well as the splitting caused by this interaction.

The dispersion relation (A2) enables yet one class of guided modes, with frequencies above ω_L. However, these frequencies are much higher than the phonon frequencies, and e.g., at $\kappa=0.01g_0$ the lowest allowed frequency is $\omega=2.856$ eV, so these modes also could not influence the phonon spectrum.

Let us now apply our theory to the model of a Wigner crystal above a semiconductor plate. Having in mind the previous discussion, we shall calculate the interaction of the longitudinal Wigner phonon with the *p*-polarized SP mode only. By doping the semiconductor one can vary the density *N* of carriers and therefore their plasma frequency $\omega_P=4\pi Ne^2/m_c$, where m_c is the effective carrier mass. Within the Drude model, one can describe the interaction of the carriers with the electromagnetic field using the dielectric function (12) and setting $\omega_T=0$ and $\omega_L^2=\omega_P^2/\epsilon_\infty$, where ϵ_∞ represents the influence of the dielectric.[19] The problem is that one usually cannot neglect losses in a semiconductor and they are described by an imaginary part of ϵ. Since our theory is developed for real ϵ, the following results will show some general features of the Wigner-phonon–SP interaction more in a qualitative way.

In that sense, we shall calculate the frequencies of a Wigner crystal in a vacuum ($\epsilon_h=1$) from the Bonsall-Maradudin model,[6] neglecting the influence of the image potential from the substrate and the perpendicular delocalization of Wigner electrons. The two-dimensional crystal is obtained in our model by setting $u(z)=\delta(z)$, i.e., $a\to\infty$ or $z_0\to0$, Eq. (2). We shall take again the lattice parameter $r_0=50$ Å so that we can compare Fig. 4 with Figs. 2 and 3. The comparison, as expected, shows only a small difference between the phonon curves.[6] The SP curves are determined for a $d_i=100$ Å thick Si layer ($\epsilon_\infty=11.7$), deposited on a metallic substrate. We have chosen three characteristic frequencies ω_L, shown in Fig. 4. The asymptotic SP frequencies

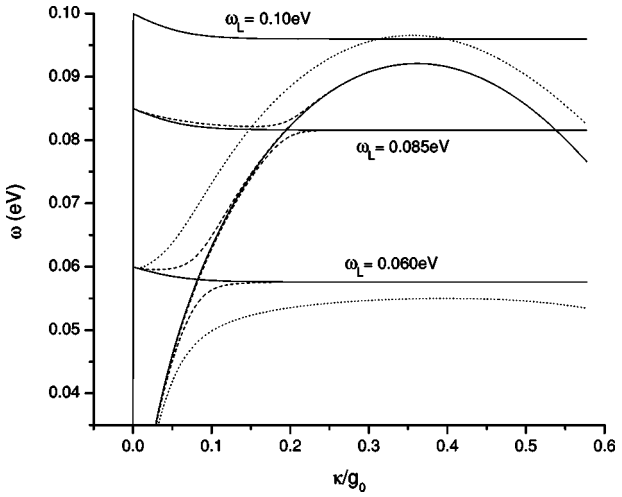

FIG. 4. Wigner crystal on a semiconductor.

$(k \gg k_L)$ are determined as $\omega_a^2=[\epsilon_\infty/(\epsilon_\infty+1)]\omega_L^2$. In semiconductors we have typically $\epsilon_\infty \gg 1$, which gives $\omega_a \approx \omega_L$. Since the Wigner-phonon–SP interaction is important only at $k \gg k_L$, i.e., at $\omega_{p\mathbf{k}}^{\beta} \approx \omega_a$, we can say that the curves shown in Fig. 4 should be typical for many semiconductors with the given frequencies ω_L.

The interaction of the SP mode with the Wigner crystal, at a distance $d_h=100$ Å above the Si layer, is shown in Fig. 4 by dashed curves. At $\omega_L=0.1$ eV there is no crossing between the SP and phonon curves, so the interaction is quite negligible. At $\omega_L=0.085$ eV there are two crossing points, but the interaction is significant only in the vicinity of the first crossing point at smaller wave vector κ, because the interaction matrix element (13) becomes exponentially damped for large κ. At lower SP frequencies ($\omega_L=0.060$ eV), the crossing occurs even at lower wave vectors so the splitting between the SP and phonon curves becomes more pronounced. Obviously, the interaction between the surface polaritons and Wigner phonons should increase with the decreasing distance between the Wigner electrons and the dielectric. Dotted lines on Fig. 4 show very large splitting in the case when this distance is reduced to 20 Å.

Let us add two additional remarks: (i) By setting $\epsilon_m=-\infty$ we have neglected SP field connected with the dynamics of conducting electrons in the metallic substrate. It can be included by taking a more realistic form of a metallic dielectric constant, e.g., $\epsilon_m=1-\omega_P^2/\omega^2$, as discussed in Sec. II C. This will bring two new SP modes associated with the metallic-dielectric interface, with the asymptotic frequencies determined from $(\epsilon_i+\epsilon_m)=0$. As expected, these modes interact very weakly with the Wigner phonons, so the dispersion relation shown on Figs. 3 and 4 remains unchanged. (ii) We did not discuss the influence of the *s*-polarized modes on the transverse Wigner phonon. The reason is that there is no *s*-polarized SP modes [see Eq. (A3) in the Appendix], while the interaction of *s*-polarized guided modes, Eq. (A4), with the transverse Wigner phonon is negligible. This means that the dispersion of the transverse Wigner phonon is not affected by the polariton field.

IV. CONCLUSION

In this article we have analyzed the interaction between electrons in the Wigner crystal, surface polaritons, and ripplons, where SP's represent the interaction of the electromagnetic field with optical phonons or plasmons in a dielectric media. All those interactions are put together to give the dispersion relation of the phonons in the Wigner lattice. There is a significant energy gap between the high-frequency SP and low-frequency ripplon spectrum, so they can be analyzed separately. The phonon-ripplon interaction is well known, so here we concentrated on higher phonon energies that include the phonon-polariton interaction. Since the energies of the conducting electrons in metallic substrate are much higher than the energies of the electrons in a Wigner crystal, we have taken a thin dielectric layer which optically active modes have the same frequency range as the Wigner phonons, and put it above a metallic substrate (an electrode).

First, we have taken an ionic crystal with well-defined optical phonons and calculated the renormalized Wigner phonon frequencies by taking into account the contribution from all polariton modes. It turns out that the only significant interaction occurs between longitudinal Wigner phonons and *p*-polarized surface polaritons. As another example, we have put Wigner electrons above a doped semiconductor layer and tuned doped carriers to obtain plasmon frequencies comparable with frequencies of longitudinal Wigner phonons. By determining the splitting between the renormalized SP and phonon curves, we have shown that this splitting can be significantly increased by decreasing either the plasmon frequency or the distance between the Wigner crystal and the dielectric surface.

The measuring of the dispersion curves splitted due to the phonon-ripplon interaction at very low frequencies[2] gave us positive evidence that the Wigner crystal really exists. Here we predict a strong splitting between the phonon and SP dispersion curves at higher frequencies, appropriate for the SP excitation; so measuring the SP spectrum could also give clear evidence of the existence of the Wigner crystal.

APPENDIX: SP DISPERSION RELATION

In this appendix we shall briefly discuss the dispersion relation of surface polaritons. Our geometry, discussed in Sec. II, consists of a thin (optically active) dielectric layer with a dielectric constant ϵ_i, above a perfectly screening metallic substrate ($\epsilon_m=-\infty$). Using the geometry shown on Fig. 1, we shall assume $\epsilon_h=\epsilon_0=1$ (vacuum) for the space above the dielectric. (If we would take precisely $\epsilon_h=1.057$ for the He layer, we would obtain much more complicated dispersion relations than given below, and without any influence on the calculated dispersion curves.) Here we are interested in the modes whose fields are damped above the dielectric layer $\bar{z}>0$, where $\bar{z}=z+d_h$ is the renormalized coordinate. The polariton eigenmodes[18] and dispersion relations[20] are determined by the parameters $\alpha_i^2=k^2-\epsilon_i\omega_{\beta\kappa}^2/c^2$ and $\alpha_0^2=k^2-\epsilon_0\omega_{\beta\kappa}^2/c^2$.

For p polarization,

$$\mathbf{A}^{\beta}_{p\mathbf{k}}(\bar{z}) = C^{\beta}_{p} \times \begin{cases} (-i\alpha_0\hat{\mathbf{k}} + k\hat{\mathbf{z}})e^{-\alpha_0 z}, & \bar{z} > 0 \\ \left(\dfrac{\epsilon_0}{\epsilon_i}\right)\left[(i\alpha_i\hat{\mathbf{k}} + k\hat{\mathbf{z}})\dfrac{e^{\alpha_i z}}{(1+e^{-2\alpha_i d_i})} + (-i\alpha_i\hat{\mathbf{k}} + k\hat{\mathbf{z}})\dfrac{e^{-\alpha_i z}}{(1+e^{2\alpha_i d_i})}\right], & -d_i < \bar{z} < 0. \end{cases}$$

(i) $\alpha_i^2 > 0$ (surface modes):

$$\frac{\alpha_0\epsilon_i}{\alpha_i\epsilon_0} = -\tanh(\alpha_i d_i). \tag{A1}$$

(ii) $\beta_i^2 = -\alpha_i^2 > 0$ (guided modes):

$$\frac{\alpha_0\epsilon_i}{\beta_i\epsilon_0} = \tan(\beta_i d_i) \tag{A2}$$

For s polarization,

$$\mathbf{A}^{\beta}_{s\mathbf{k}}(\bar{z}) = C^{\beta}_{s}(\hat{\mathbf{k}} \times \hat{\mathbf{z}}) \times \begin{cases} e^{-\alpha_0 z}, & \bar{z} > 0 \\ \dfrac{e^{-i\beta_i z}}{1-e^{i2\beta_i d_i}} + \dfrac{e^{i\beta_i z}}{1-e^{-i2\beta_i d_i}}, & -d_i < \bar{z} < 0. \end{cases}$$

(i) $\alpha_i^2 > 0$ (surface modes):

$$\frac{\alpha_i}{\alpha_0} = -\tanh(\alpha_i d_i), \text{ no solution}. \tag{A3}$$

(ii) $\beta_i^2 = -\alpha_i^2 > 0$ (guided modes):

$$\frac{\beta_i}{\alpha_0} = -\tan(\beta_i d_i). \tag{A4}$$

To determine the coefficients C^{β}_{ν} we shall use the theory developed in Ref. 15, which takes into account both the space and the frequency dependence of the dielectric constant. The eigenmodes normalization is given by

$$\int dz\tilde{\epsilon}(z)|\mathbf{A}^{\beta}_{\nu\mathbf{k}}(z)|^2 = 1, \tag{A5}$$

where the renormalized dielectric constant is

$$\tilde{\epsilon}(z) = \frac{\partial\,\omega^2\epsilon(z)}{\partial\,\omega^2}.$$

Obviously, $\tilde{\epsilon}_0 = \epsilon_0 = 1$, and from Eq. (12):

$$\tilde{\epsilon}_i = \epsilon_\infty + \epsilon_\infty\frac{(\omega_L^2 - \omega_T^2)\omega_T^2}{(\omega_T^2 - \omega^2)^2}.$$

Inserting the eigenmodes $\mathbf{A}^{\beta}_{\nu\mathbf{k}}(\bar{z})$ into Eq. (A5) we find

$$|C^{\beta}_{p}|^{-2} = \frac{k^2+\alpha_0^2}{2\alpha_0} + \left(\frac{\epsilon_0}{\epsilon_i}\right)^2\frac{\tilde{\epsilon}_i}{2\alpha_i}\{(k^2+\alpha_i^2)\tanh(\alpha_i d_i) + (k^2-\alpha_i^2) \times [1-\tanh^2(\alpha_i d_i)]\alpha_i d_i\}, \quad \alpha_i^2 > 0$$

$$|C^{\beta}_{p}|^{-2} = \frac{k^2+\alpha_0^2}{2\alpha_0} + \left(\frac{\epsilon_0}{\epsilon_i}\right)^2\frac{\tilde{\epsilon}_i}{2\beta_i}\{(k^2-\beta_i^2)\tan(\beta_i d_i) + (k^2+\beta_i^2) \times [1+\tan^2(\beta_i d_i)]\beta_i d_i\}, \quad \beta_i^2 > 0$$

$$|C^{\beta}_{s}|^{-2} = \frac{1}{2\alpha_0} + \frac{\tilde{\epsilon}_i}{2\beta_i}\left\{\frac{\alpha_0}{\beta_i} + \left[1+\left(\frac{\alpha_0}{\beta_i}\right)^2\right]\beta_i d_i\right\}, \quad \beta_i^2 > 0.$$

[1] E. P. Wigner, Phys. Rev. **46**, 1002 (1934).
[2] C. C. Grimes and G. Adams, Phys. Rev. Lett. **42**, 795 (1979).
[3] D. S. Fisher, B. I. Halperin, and P. M. Platzman, Phys. Rev. Lett. **42**, 798 (1979).
[4] E. Y. Andrei, *Two-Dimensional Electron Systems on Helium and Other Cryogenic Substrates* (Kluwer Academic, Dordrecht, 1997).
[5] C. C. Grimes, T. R. Brown, M. L. Burns, and C. L. Zipfeld, Phys. Rev. B **13**, 140 (1976); Z. Lenac and M. Šunjić, Phys. Rev. B **48**, 14 496 (1993).
[6] L. Bonsall and A. A. Maradudin, Phys. Rev. B **15**, 1959 (1977); Z. Lenac and M. Šunjić, Phys. Rev. B **44**, 11 465 (1991).
[7] F. M. Peeters, Phys. Rev. B **30**, 159 (1984); Z. Lenac and M. Šunjić, *ibid.* **46**, 7821 (1992).
[8] B. Tanatar and D. M. Ceperley, Phys. Rev. B **39**, 5005 (1989).
[9] Z. Lenac and M. Šunjić, Phys. Rev. B **59**, 6752 (1999).
[10] S. Orozco, R. M. Mendez-Moreno, and M. Moreno, Phys. Rev. B **67**, 195109 (2003); see Refs. 13–18 in Ref. 9.
[11] D. Marty and J. Pointrenaud, J. Phys. (France) **45**, 1243 (1984).
[12] D. C. Glattli, E. Y. Andrei, and F. I. B. Williams, Surf. Sci. **196**, 17 (1988); M. D'Iorio, V. M. Pudalov, S. V. Kravchenko, and J. W. Campbell, *ibid.* **305**, 115 (1994).
[13] M. Haque, I. Paul and S. Pankov, Phys. Rev. B **68**, 045427 (2003).
[14] R. J. Glauber and M. Lewenstein, Phys. Rev. A **43**, 467 (1991).
[15] Z. Lenac, Phys. Rev. A **68**, 063815 (2003).
[16] J. J. Hopfield, Phys. Rev. **182**, 945 (1969).
[17] V. Savona, Z. Hradil, A. Quattropani, and P. Schwendimann, Phys. Rev. B **49**, 8774 (1994); S. Jorda, *ibid.* **50**, 2283 (1994).
[18] Z. Lenac, Phys. Rev. A **63**, 033815 (2001).
[19] M. van Exter and D. Grischkowsky, Phys. Rev. B **41**, 12 140 (1990).
[20] K. L. Kliewer and R. Fuchs, Adv. Chem. Phys. **27**, 355 (1974).